Supporting Information for

Facilitated Electron Transfer by Mn dopants in 1-Dimensional CdS Nanorods for Enhanced Photocatalytic Hydrogen Generation

*Walker MacSwain,[a] Hanjie Lin,[a] Zhi-Jun Li,[a] Shuya Li,[a] Chun Chu,[a] Lacie Dube,[b] Ou Chen,[b] Gyu Leem,[c,d] Weiwei Zheng.[a,]**

[a] Department of Chemistry, Syracuse University, Syracuse, New York 13244, United States

[b] Department of Chemistry, Brown University, Providence, Rhode Island, 02912, United States.

[c] Department of Chemistry, State University New York College of Environmental Science Forestry, Syracuse, New York 13210, United States

[d] The Michael M. Szwarc Polymer Research Institute, 1 Forestry Drive, Syracuse, New York 13210, United States

Table of Contents

I. Experimental Details

Chemicals. Zinc diethyldithiocarbamate ($Zn(DDTC)_2$, 98% Sigma-Aldrich), oleylamine (OAm, 70%, Sigma-Aldrich), 1-octadecene (ODE, 90%, Alfa-Aesar), oleic acid (OA, 90%, Sigma-Aldrich), 1, 2-dichlorobenzene (≥99%, Sigma-Aldrich), diphenyl ether (≥99%, Sigma-Aldrich), 1, 2-hexanedecanediol (90%, Sigma-Aldrich), hexane (99%, EMD), ethanol (≥99%, anhydrous, Pharmco) and platinum(II) acetylacetonate (≥99.98%, Sigma-Aldrich). All chemicals were used as purchased without further purification.

A. Synthesis of 1D Mn:CdS/ZnS and Mn:CdS-Pt/ZnS core/shell NRs. Core/shell nanorods were synthesized according to a slightly modified literature procedure.[1, 2] Typically, the as-purified 1D Mn:CdS or Mn:CdS-Pt NRs were dissolved in 9 mL ODE and 3 mL OAm. After that 228 mg (0.63 mmol) of $Zn(DDTC)_2$ was added to the NR (0.45 mmol) solution in a three-neck flask and was vacuumed from room temperature to 80°C and kept vacuuming at 80°C for additional 1.5 hours. Under Ar flow, the reaction solution was heated to a target growth temperature at 220 °C for 1.5 hours. At the end of the reaction, the solution was removed from the heating mantle and allowed to cool to approximately 60 °C. The core/shell NRs were separated from the crude solution by precipitating the particles with ethanol and centrifuging. The precipitate was further purified once by resuspending the NRs in hexane and then reprecipitating with ethanol and centrifugation.

B. Synthesis of 1D hybrid CdS-Pt NRs. 1D CdS-Pt NRs were synthesized based on a slightly modified literature reference.[3] First, 0.2 mL OA, 0.2 mL OAm, and 43.0 mg (0.17 mmol) of 1,2-hexadecanediol were heated in 9 mL diphenyl ether at 80 °C under vacuum for 30 min to remove traces of water. The optical density (OD) of the CdS-based NR stock solution can be measured by diluting the stock solution of NRs (100 µL into 1 mL *i.e.,* 100x dilution) and the OD of the NR stock solution can be calculated by the absorbance of the diluted solution multiplied by 100. 65.5 mg (0.17 mmol) Pt acetylacetonate was added to the suspension of the synthesized CdS stock solution (OD = 20) in 3 mL of 1, 2 dichlorobenzene and sonicated at 65 °C for 10 min to promote dissolution of the Pt precursor. The reaction mixture was purged with Ar and heated to 200 °C before injecting the 3 mL suspension of Pt precursor and NRs. Typically, after 10 minutes the reaction was removed from heat and quenched in a water bath. The product was washed by precipitation in ethanol followed by centrifugation. The precipitate was further purified twice by resuspending the NRs in hexane and then reprecipitating with ethanol and centrifuging.

II. Characterization of 1D CdS-based NRs

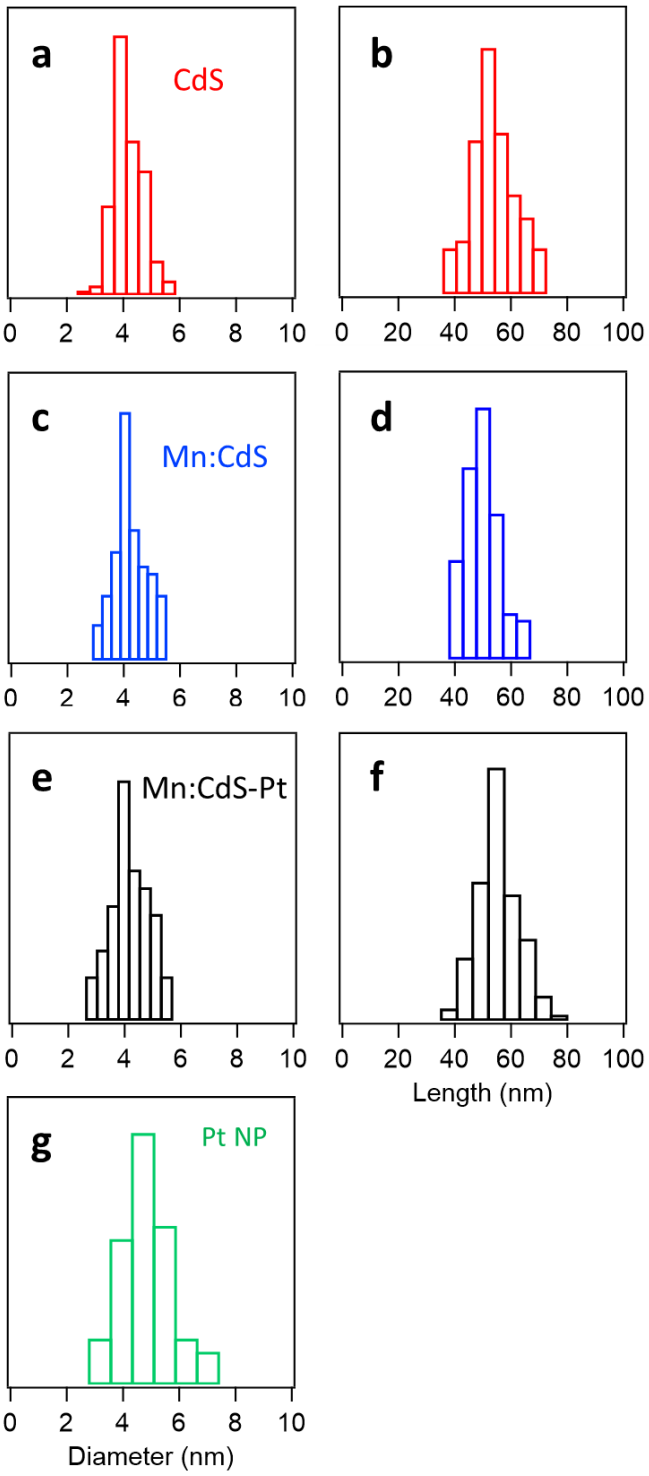

Figure S1. Histograms of the diameter and length of 1D CdS (a-b), Mn:CdS (c-d), and Mn:CdS-Pt (e-f) NRs. g) Histogram of the diameter of the Pt NP tips on the Mn:CdS-Pt NRs.

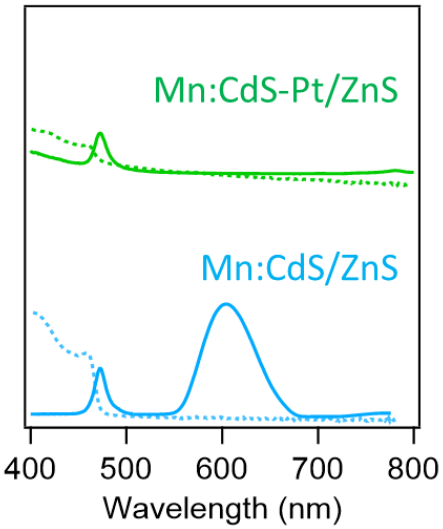

Figure S2. Absorbance (dashed lines) and PL spectra (solid lines) of ZnS shelled Mn:CdS/ZnS and Mn:CdS-Pt/ZnS core/shell NRs.

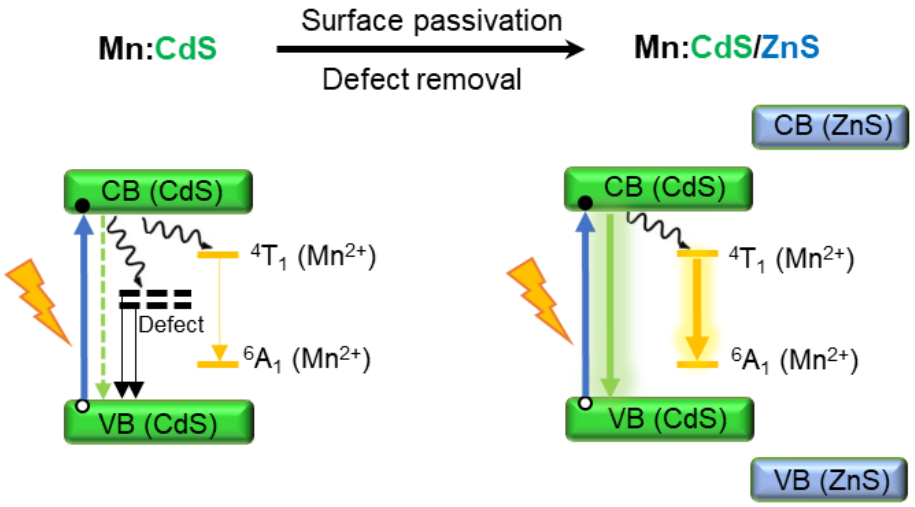

Figure S3. ZnS Shell passivation for type I Mn:CdS/ZnS core/shell NCs with high CdS host and Mn^{2+} dopant PL intensity by the removal of surface defects/trap states. In the Type I system, the bandgap of the core material (CdS) is smaller than the bandgap of the shell material (ZnS) with the excited electrons and holes confined inside the CdS core.[4]

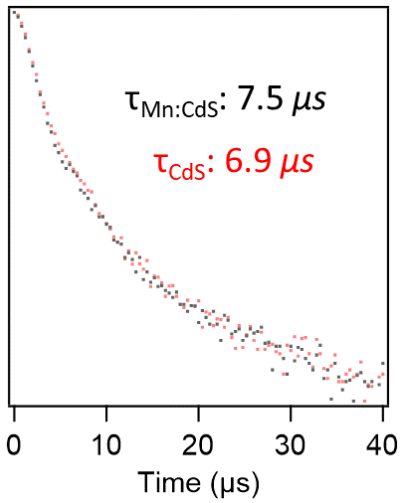

Figure S4. PL decay of Mn:CdS and CdS NRs (monitored at 600 nm). The decay times of the defect/Mn emission at 600 nm are 7.5 μs and 6.9 μs for Mn:CdS and CdS NRs, respectively.

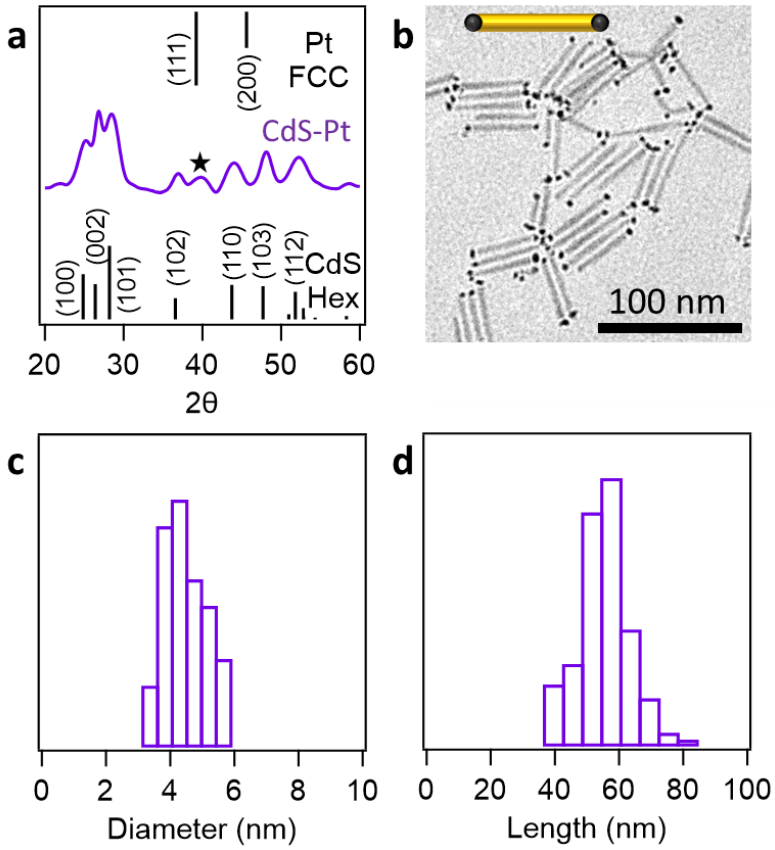

Figure S5. Structural and morphology characterization of the CdS-Pt NRs. a) the powder XRD pattern of CdS-Pt NRs (★ indicates the diffraction peak from Pt). b) the TEM, c) histogram of the diameter and d) histogram of the length of CdS-Pt NRs.

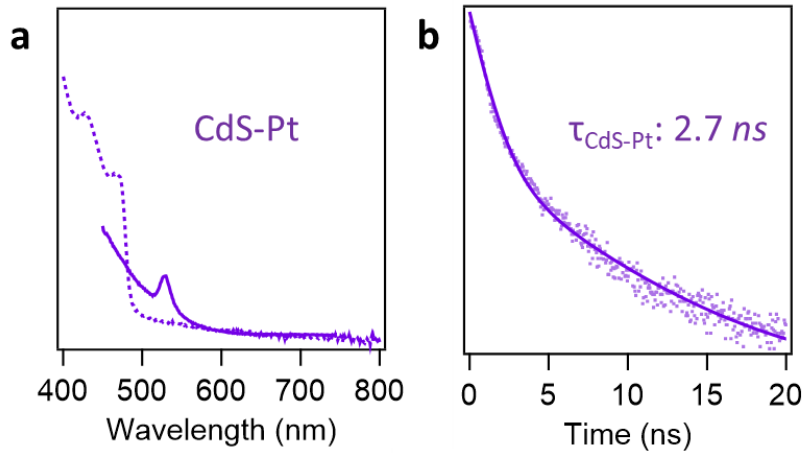

Figure S6. a) Normalized absorbance and emission spectra of CdS-Pt NRs and b) PL decays of the CdS of 1D CdS-Pt NRs.

III. Electrochemical Measurements.

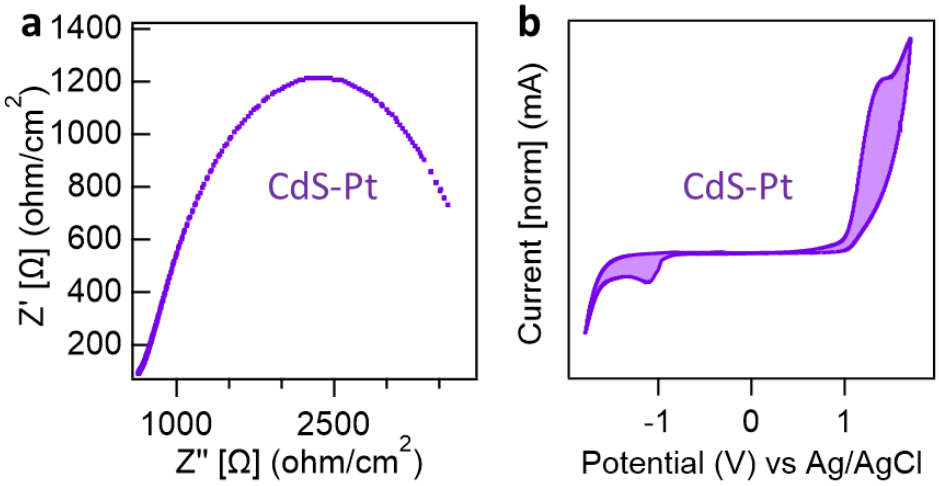

Figure S7. a) EIS (Nyquist plot) of and b) Normalized cyclic voltammetry spectra of 1D CdS-Pt NRs.

Table S1. The bandgaps and bandedge positions of the valence and conduction bands of the NRs.

	CdS	CdS-Pt	Mn:CdS	Mn:CdS-Pt
Bandgap	2.7	2.6	2.6	2.6
VB	1.5	1.4	1.4	1.4
CB	-1.2	-1.2	-1.2	-1.2

Note: The oxidation potentials are calculated from the CV, while the reduction potentials are calculated from Tauc plots of the absorbance spectra.

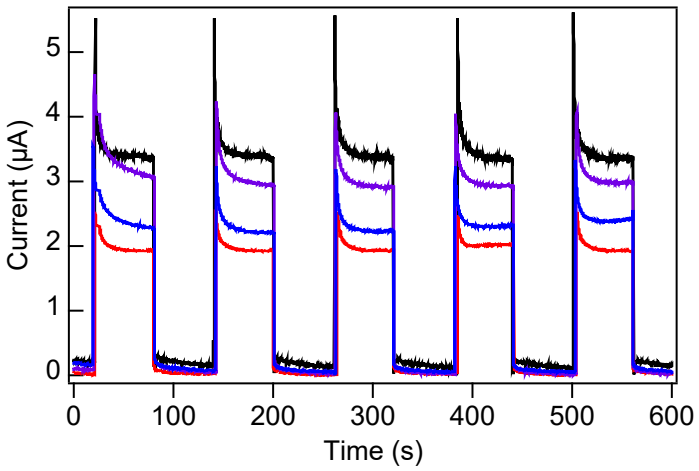

Figure S8. Photocurrent responses to on-off illumination of the CdS NRs (red), Mn:CdS NRs (blue), CdS-Pt NRs (purple), and Mn:CdS-Pt NRs (black) electrodes.

IV. Internal Quantum Efficiency (IQE) Calculations

The photochemical reactions for IQE were performed using a solar simulator (AM1.5G, 100 mW/cm^2, Newport 91160) irradiating the 4.8 cm^2 surface of the centrifuge tube reactor under striring at 1000 rpm. The volume of the generated H_2 gas was collected in a burette and recorded every 15 minutes. For example, the Mn:CdS-Pt NRs generated 6.8 mL under solar simulated irradiation for 1 hr. Internal quantum efficiency can be defined as the ratio between the charge utilization of a photocatalytic system divided by the number of photons that reach the cell's surface.[5] The relationship of quantum efficiency to photocatalytic water splitting is defined in equation 1 and 2.

$$QE(\%) = \frac{reacted\ electrons}{incident\ photons} \times 100\%\ \textit{(Eq. 1)}$$

$$QE(\%) = \frac{\#\ of\ H_2\ molecules \times 2}{incident\ photons} \times 100\%\ \textit{(Eq. 2)}$$

The QE ratio can mathematically be described then by equation 3 where the ΔG^0 (J mol^{-1}) as the standard Gibbs free energy for the formation of H_2 molecules, R (mol s^{-1}) as the rate of generation of H_2 molecules, E_s (J s^{-1} m^{-2}) as the incident photons, and A (m^2) as the irradiated area of the photochemical system.[6]

$$QE(\%) = \frac{\Delta G^0 R}{E_s A} \times 100\%\ \textit{(Eq. 3)}$$

ΔG can be obtained from the Equation 4 below, which is the Nernst equation where n is the number of electrons transferred in the reaction, F (C mol^{-1}) is Faraday's constant, and E (V) is the potential difference.

$$\Delta G = -nFE\ \textit{(Eq.4)}$$

Finally, the IQE can be calculated by combining equations 2-4, given that the potential of photocatalytic water splitting is -1.23 V, the photocatalytic system has 0.151 W/cm^2 of photon irradiation of which the CdS based NRs can only absorb ~20% of the total irradiation (Figure 2a in the main manuscript), the area irradiated is 4.87 cm^2, and the rate can be calculated by converting the moles of hydrogen generated into a rate of mol per second. The as calculated internal quantum efficiencies are given in Figure S7 below.

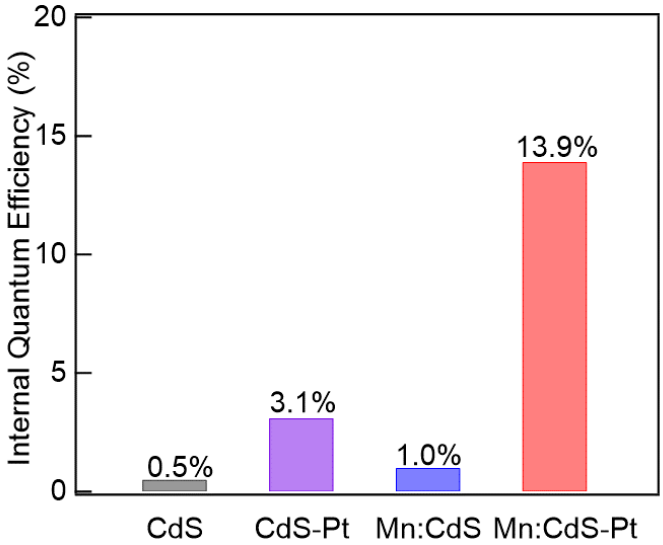

Figure S9. The experimentally measured internal quantum efficiencies of the 1D CdS, CdS-Pt, Mn:CdS, and Mn:CdS-Pt NRs.

V. Photocatalytic Water Splitting Studies

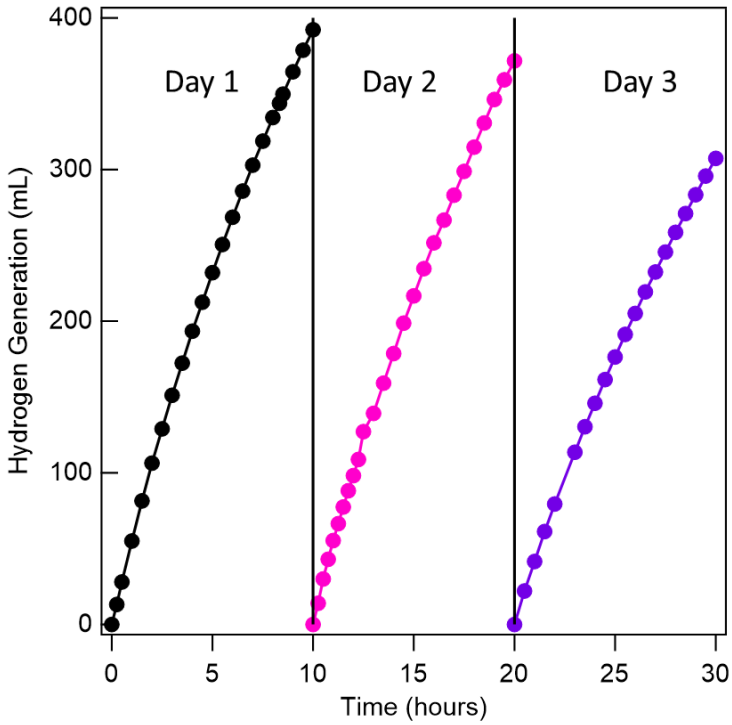

Figure S10. Long-term recycle studies for the 1D Mn:CdS-Pt NR-based photocatalytic system. The photochemical system was allowed to react for a cycle of 10 hours, then the photocatalyst was recollected by centrifugation, the solution remade with fresh reactants, and allowed to react again for 10 hours in the next cycle.

Table S2. Concentration of Cd (mg/L) of the initial and final photocatalytic solution, as well as the supernatant after each cycle test measured by ICP-OES.

	Initial Solution	Supernatant Cycle 1	Supernatant Cycle 2	Supernatant Cycle 3	Supernatant Cycle 4	Final Solution
[Cd] (mg/L)	0.91	0.039	0.035	0.034	0.032	0.73

Elemental analysis of the supernatant of the photocatalytic solution during the centrifugation step between cycles was performed by ICP-OES to detect the concentration of Cd ions. The trace amount of Cd in the supernatant should be due to the wash losses of the NRs since it is impossible to recollect all NRs from centrifugation, as well as the possible photodegradation during the photocatalytic reactions. Since there are no significant changes in absorption peak position before and after photocatalytic reactions, no significant change in the size of the NRs is expected. Therefore, the wash and the possible photodegradation losses might be the main reason of the decreased photocatalytic performance of H_2 generation (~6% per cycle).

The initial concentration of Cd-ions in the photocatalytic solution from the amount of Mn:CdS-Pt NRs added into the photocatalytic solution was measured as 0.91 mg/L from ICP-OES. The [Cd] from collected supernatants after each cycle test is shown in Table 1, which indicates on average ~4.1% sample loss for each cycle due to wash losses and possible photodegradation. The average ~4.1% sample loss for each cycle is very close to the ~6% decrease of photocatalytic performance of H_2 generation per cycle, but with a slightly smaller value. It should be noted that after the centrifugation/cleaning process for each cycle, the samples were pipetted back to a glass tube for the next cycle test. The transfer of the NRs to and from the glass tube could also lead to the loss of trace amount of NR sample. To verify the transfer losses, we measured the [Cd] of the photocatalytic solution in the last cycle (5^{th} cycle in the measurement), which was found to be 0.73 mg/L. The [Cd] in the photocatalytic solution in the last cycle is ~0.77 mg/L calculated from the loss of [Cd] in the supernatant of each cycle (*i.e.,* subtract the sum of the [Cd] in the supernatant cycles from 0.91 mg/L). The slightly smaller [Cd] in the final photocatalytic solution than that from the calculation of wash/photodegradation losses support the additional losses from sample transfer between centrifuge tubes and the glass tubes for photocatalytic reactions. Therefore, the sample losses from wash, transfer, and photodegradation contribute to the ~6% decrease of photocatalytic performance of H_2 generation per cycle.

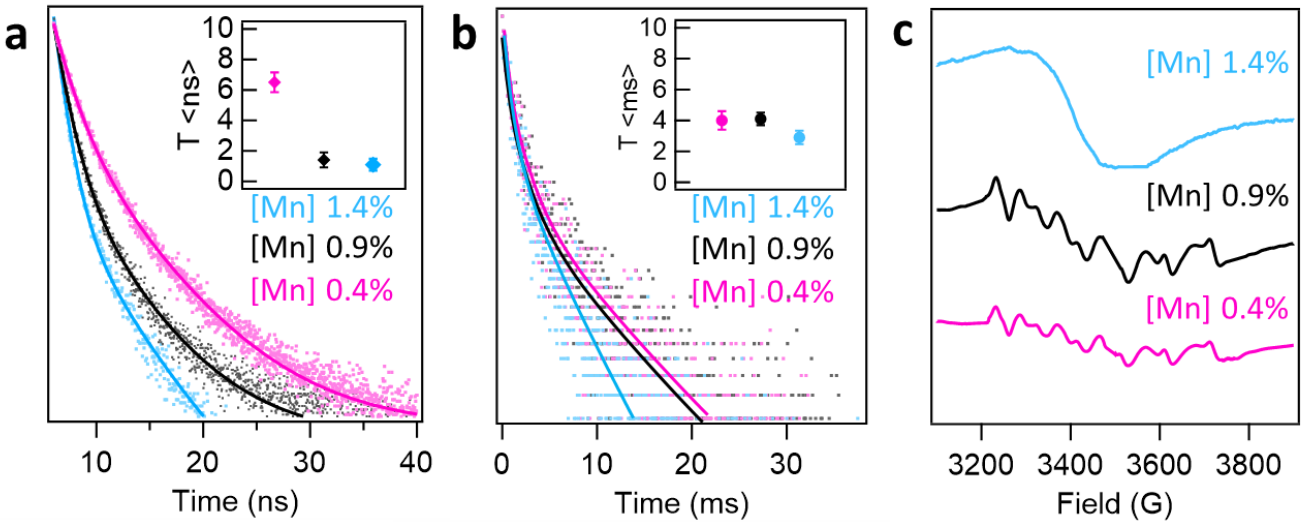

Figure S11. Mn^{2+} dopant concentration (0.4 - 1.4%) -dependent studies for the 1D Mn:CdS-Pt NR-based photocatalysts. a) CdS band edge PL lifetime and calculated lifetimes inset, b) Mn^{2+} dopant lifetimes of Mn:CdS/ZnS core/shell NRs with calculated lifetimes inset, and c) EPR spectra of the NRs with different doping concentration.

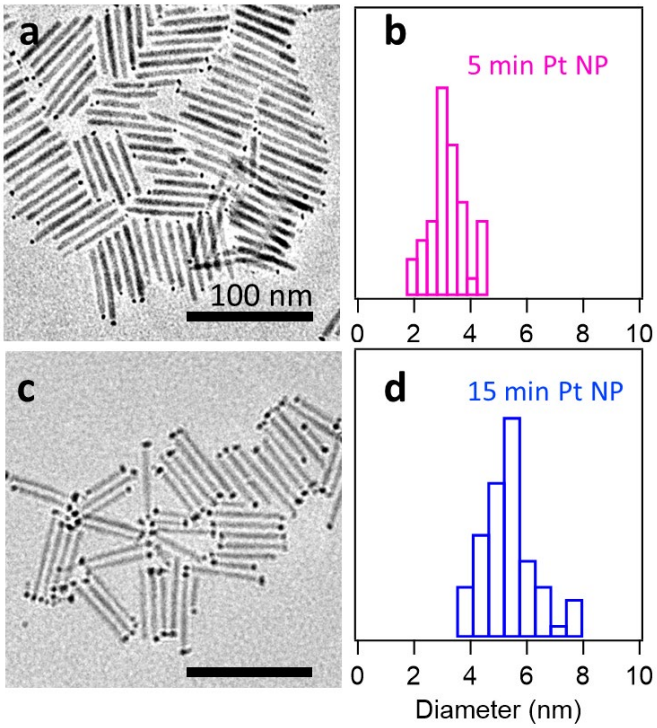

Figure S12. Pt reaction time-dependent studies of the Mn:CdS-Pt NR-based photocatalysts. a) TEM and b) histogram of the Pt NP diameter of 1D Mn:CdS-Pt NRs with 5 minutes Pt tipping reaction time. c) TEM and d) histogram of the Pt NP diameter of 1D Mn:CdS-Pt NRs with 15 minutes Pt tipping reaction time.

Table S3. Summary of reported CdS-based photocatalysts which utilize Pt as a cocatalyst.

Photocatalyst	Co-catalyst	Light Source (W/nm)	Sacrificial Reagent	Rate (μmol/h/g)	IQE (%)	Reference
CdS nanowire	Pt	500 Hg/<400	Na_2S/Na_2SO_3	60	-	[7]
Hexagonal CdS	Pt	300 Xe/≥420	Na_2S/Na_2SO_3	1,600	-	[8]
Nanoporous CdS	Pt	300 Xe/≥420	Na_2S/Na_2SO_3	600	-	[9]
Mesoporous	Pt	400 Hg	Na_2S/Na_2SO_3	14,150	-	[10]
CdS microcrystal	Pt	500 Xe/≥400	Na_2S/Na_2SO_3	4,600	-	[11]
CdS-$AgGaS_2$	Pt	450 Hg/≥420	Na_2S/Na_2SO_3	2,960	-	[12]
Ag_2S/CdS	Pt	Hg-Xe/>400	Na_2S/Na_2SO_3	870	-	[13]
CdS/GR	Pt	350 Xe/≥420	Lactic Acid	56,000	-	[14]
CdS/TiO_2 Nanotube	Pt	300 Xe/≥420	Na_2S/Na_2SO_3	2,080	0.84	[15]
CdS/TiO_2	Pt	450 Hg/≥420	Na_2S/Na_2SO_3	6,720	-	[16]
CdS/TaON	Pt	300 Xe/=420	Na_2S/Na_2SO_3	3,161	-	[17]
CdS/TNT	Pt	500 Xe/≥430	Na_2S/Na_2SO_3	1,761	0.12	[18]
CdS/Re cellulose	Pt	250 Xe/≥420	Na_2S/Na_2SO_3	1,320	-	[19]
CdS/zeolite	Pt	400 Hg UV	Na_2S/Na_2SO_3	6,000	-	[20]
ZnO-CdS@Cd	Pt	300 Xe	Na_2S/Na_2SO_3	19,200	-	[21]
$Ni(OH)_2$/CdS	Pt	300 Xe/≥420	Triethylamine	5,080	-	[22]
CdS/g-C_3N_4	Pt	300 Xe/≥420	MeOH	4,152	-	[23]
CdS QD's/g-C_3N_4	Pt	300 Xe/≥400	MeOH	17	-	[24]
WS_2/CdS	Pt	300 Xe/≥400	Lactic Acid	4,200	-	[25]
GO/CdS	Pt	350 Hg/>420	-	1,120	-	[26]
Al_2O_3@CdS	Pt	Xe/≥420	-	62	-	[27]
Mn:CdS	**Pt**	**LEDs/=405**	**IPA/Acetone**	**287,000**	**13.9**	**This work**

References.

1. Hofman, E.; Khammang, A.; Wright, J. T.; Li, Z.-J.; McLaughlin, P. F.; Davis, A. H.; Franck, J. M.; Chakraborty, A.; Meulenberg, R. W.; Zheng, W. Decoupling and Coupling of the Host–Dopant Interaction by Manipulating Dopant Movement in Core/Shell Quantum Dots. *J. Phys. Chem. Lett.* 2020, **11**, (15), 5992-5999.

2. Davis, A. H.; Hofman, E.; Chen, K.; Li, Z.-J.; Khammang, A.; Zamani, H.; Franck, J. M.; Maye, M. M.; Meulenberg, R. W.; Zheng, W. Exciton Energy Shifts and Tunable Dopant Emission in Manganese-Doped Two-Dimensional CdS/ZnS Core/Shell Nanoplatelets. *Chem. Mater.* 2019, **31**, (7), 2516-2523.

3. Habas, S. E.; Yang, P.; Mokari, T. Selective Growth of Metal and Binary Metal Tips on CdS Nanorods. *J. Am. Chem. Soc.* 2008, **130**, (11), 3294-3295.

4. Reiss, P.; Protiere, M.; Li, L. Core/Shell semiconductor nanocrystals. *Small* 2009, **5**, (2), 154-68.

5. Zhang, J.; Yu, J.; Jaroniec, M.; Gong, J. R. Noble Metal-Free Reduced Graphene Oxide-$Zn_xCd_{1-x}S$ Nanocomposite with Enhanced Solar Photocatalytic H_2-Production Performance. *Nano Lett.* 2012, **12**, (9), 4584-4589.

6. Murugan, A. V.; Muraliganth, T.; Manthiram, A. Rapid, Facile Microwave-Solvothermal Synthesis of Graphene Nanosheets and Their Polyaniline Nanocomposites for Energy Strorage. *Chem. Mater.* 2009, **21**, (21), 5004-5006.

7. Jang, J. S.; Joshi, U. A.; Lee, J. S. Solvothermal Synthesis of CdS Nanowires for Photocatalytic Hydrogen and Electricity Production. *J. Phys. Chem. C* 2007, **111**, (35), 13280-13287.

8. Bao, N.; Shen, L.; Takata, T.; Domen, K.; Gupta, A.; Yanagisawa, K.; Grimes, C. A. Facile Cd−Thiourea Complex Thermolysis Synthesis of Phase-Controlled CdS Nanocrystals for Photocatalytic Hydrogen Production under Visible Light. *J. Phys. Chem. C* 2007, **111**, (47), 17527-17534.

9. Bao, N.; Shen, L.; Takata, T.; Domen, K. Self-Templated Synthesis of Nanoporous CdS Nanostructures for Highly Efficient Photocatalytic Hydrogen Production under Visible Light. *Chem. Mater.* 2008, **20**, (1), 110-117.

10. Sathish, M.; Viswanath, R. P. Photocatalytic generation of hydrogen over mesoporous CdS nanoparticle: Effect of particle size, noble metal and support. *Catal. Today* 2007, **129**, (3-4), 421-427.

11. Muruganandham, M.; Kusumoto, Y.; Okamoto, C.; Muruganandham, A.; Abdulla-Al-Mamun, M.; Ahmmad, B. Mineralizer-Assisted Shape-Controlled Synthesis, Characterization, and Photocatalytic Evaluation of CdS Microcrystals. *J. Phys. Chem. C* 2009, **113**, (45), 19506-19517.

12. Shen, Z.; Chen, G.; Wang, Q.; Yu, Y.; Zhou, C.; Wang, Y. Sonochemistry synthesis and enhanced photocatalytic H_2-production activity of nanocrystals embedded in CdS/ZnS/In_2S_3 microspheres. *Nanoscale* 2012, **4**, (6), 2010-2017.

13. Shen, S.; Guo, L.; Chen, X.; Ren, F.; Mao, S. S. Effect of Ag_2S on solar-driven photocatalytic hydrogen evolution of nanostructured CdS. *Int. J. Hydrogen Energy* 2010, **35**, (13), 7110-7115.

14. Ye, A.; Fan, W.; Zhang, Q.; Deng, W.; Wang, Y. CdS–graphene and CdS–CNT nanocomposites as visible-light photocatalysts for hydrogen evolution and organic dye degradation. *Catal. Sci. Technol.* 2012, **2**, (5), 969-978.

15. Li, C.; Yuan, J.; Han, B.; Jiang, L.; Shangguan, W. TiO_2 nanotubes incorporated with CdS for photocatalytic hydrogen production from splitting water under visible light irradiation. *Int. J. Hydrogen Energy* 2010, **35**, (13), 7073-7079.

16. Park, H.; Choi, W.; Hoffmann, M. R. Effects of the preparation method of the ternary CdS/TiO_2/Pt hybrid photocatalysts on visible light-induced hydrogen production. *J. Mater. Chem.* 2008, **18**, (20), 2379-2385.

17. Hou, J.; Wang, Z.; Kan, W.; Jiao, S.; Zhu, H.; Kumar, R. V. Efficient visible-light-driven photocatalytic hydrogen production using CdS@TaON core–shell composites coupled with graphene oxide nanosheets. *J. Mater. Chem.* 2012, **22**, (15), 7291-7299.

18. Chen, Y.; Wang, L.; Lu, G.; Yao, X.; Guo, L. Nanoparticles enwrapped with nanotubes: A unique architecture of CdS/titanate nanotubes for efficient photocatalytic hydrogen production from water. *J. Mater. Chem.* 2011, **21**, (13), 5134-5141.

19. Ke, D.; Liu, S.; Dai, K.; Zhou, J.; Zhang, L.; Peng, T. CdS/Regenerated Cellulose Nanocomposite Films for Highly Efficient Photocatalytic H_2 Production under Visible Light Irradiation. *J. Phys. Chem. C* 2009, **113**, (36), 16021-16026.

20. Sathish, M.; Viswanathan, B.; Viswanath, R. Alternate synthetic strategy for the preparation of CdS nanoparticles and its exploitation for water splitting. *Int. J. Hydrogen Energy* 2006, **31**, (7), 891-898.

21. Wang, X.; Liu, G.; Wang, L.; Chen, Z.-G.; Lu, G. Q. M.; Cheng, H.-M. ZnO-CdS@Cd Heterostructure for Effective Photocatalytic Hydrogen Generation. *Adv. Energy Mater.* 2012, **2**, (1), 42-46.

22. Ran, J.; Yu, J.; Jaroniec, M. $Ni(OH)_2$ modified CdS nanorods for highly efficient visible-light-driven photocatalytic H_2 generation. *Green Chem.* 2011, **13**, (10), 2708-2713.

23. Ding, X.; Li, Y.; Zhao, J.; Zhu, Y.; Li, Y.; Deng, W.; Wang, C. Enhanced photocatalytic H_2 evolution over CdS/Au/g-C_3N_4 composite photocatalyst under visible-light irradiation. *APL Mater.* 2015, **3**, (10).

24. Ge, L.; Zuo, F.; Liu, J.; Ma, Q.; Wang, C.; Sun, D.; Bartels, L.; Feng, P. Synthesis and Efficient Visible Light Photocatalytic Hydrogen Evolution of Polymeric g-C_3N_4 Coupled with CdS Quantum Dots. *J. Phys. Chem. C* 2012, **116**, (25), 13708-13714.

25. Zong, X.; Han, J.; Ma, G.; Yan, H.; Wu, G.; Li, C. Photocatalytic H_2 Evolution on CdS Loaded with WS_2 as Cocatalyst under Visible Light Irradiation. *J. Phys. Chem. C* 2011, **115**, (24), 12202-12208.

26. Li, Q.; Guo, B.; Yu, J.; Ran, J.; Zhang, B.; Yan, H.; Gong, J. R. Highly efficient visible-light-driven photocatalytic hydrogen production of CdS-cluster-decorated graphene nanosheets. *J Am Chem Soc* 2011, **133**, (28), 10878-84.

27. Ning, X.; Zhen, W.; Wu, Y.; Lu, G. Inhibition of CdS photocorrosion by Al_2O_3 shell for highly stable photocatalytic overall water splitting under visible light irradiation. *Appl. Catal., B* 2018, **226**, 373-383.